Construction and Building Materials 254 (2020) 119307

Contents lists available at ScienceDirect

Construction and Building Materials

journal homepage: www.elsevier.com/locate/conbuildmat

Piezoelectric cement sensor-based electromechanical impedance technique for the strength monitoring of cement mortar

Huang Hsing Pan *, Ming-Wang Huang

Department of Civil Engineering, National Kaohsiung University of Science and Technology, Kaohsiung 80778, Taiwan

ARTICLE INFO

Article history:
Received 13 February 2020
Received in revised form 19 April 2020
Accepted 20 April 2020

Keywords:
Cement
Piezoelectric sensor
EMI
Health monitoring
Impedance spectrum
Strength

ABSTRACT

Piezoelectric cement is a 0–3 type cement-based piezoelectric composite comprising 50% lead zirconate titanate (PZT) particles. Piezoelectric cement sensors, which are based on the electromechanical impedance (EMI) technique, are applied for the structural health monitoring (SHM) of cementitious materials. The compressive strength (f_c) of three cement mortar types with water-to-cement ratios of 0.4, 0.5, and 0.6 were monitored for 56 days using an embedded piezoelectric cement sensor (PEC sensor). The PZT sensor was used as a counterpart in the experiments. The results indicate that the strength monitoring capability of the PEC sensor is similar to that of the PZT sensor. However, the monitoring capability of the PEC sensor is superior to that of the PZT sensor because the electrical impedance change of the PEC sensor is more evident. The PEC sensor is easy to find an effective monitoring frequency at which the conductance decreases with the age of the cementitious materials because it has the advantage of a broader frequency bandwidth that provides higher recognizing ability than the PZT. For the PEC sensor, a conductance root mean square deviation G_R in a high frequency region, such as that higher than 800 kHz, can promote the reliability of mortar strength monitoring. Based on the G_R value calculated at the effective monitoring frequency, the relation between f_c and G_R in the mortar presents a logarithmic behavior. The PEC sensor is suitable for monitoring the change in material properties, especially for cementitious materials.

1. Introduction

In the last two decades, many nondestructive testing (NDT) methods for structural health monitoring (SHM) have been developed in the civil engineering domain; these methods are based on the characteristics of waves, electrical, optical, acoustical, magnetic, and the mechanical properties of the tested materials [1,2]. For instance, the strength and damage evaluations of cement-based composites and structures have been conducted using ultrasonic pulse velocity (UPV) methods [3-6], optical fiber [7,8], carbon nanofiber [9], acoustic emission (AE) [10,11], vibration frequency [12,13], X-ray computed tomography (CT) [14,15], and shape memory alloy (SMA) wires for magnetic sensing [16]. Moreover, piezoelectric sensors fabricated using piezoelectric ceramics, piezoelectric polymers, and piezoelectric composites are used as sensors and actuators for SHM. Among them, lead zirconate titanate (PZT) sensors comprising PZT ceramic or smart aggregates (SAs) [17] have been widely applied to the evaluation of concrete structures; they analyze the characteristics of resistance [18,19], voltage [20,21], frequency [13], dielectric constant [22], and impedance [23,24] to assess and detect the strength and damage conditions of these structures. Reliable NDT techniques developed for real-time health monitoring of civil engineering structures are being used currently.

Piezoelectric sensors based on electromechanical impedance (EMI) technique are one of the most effective methods for SHM. In these sensors, the piezoelectric sensor simultaneously acts as a sensor and actuator [23,25]. Many studies [26–38] have conducted the damage detection of structures by using a PZT sensor with the EMI technique because of easy signal interpretation. For instance, Tawie and Lee [26] investigated the bond development at the steel–concrete interface according to the impedance change. Xu et al. [28] identified structural damage by using PZT sensors embedded and affixed on the host structures and determined the root mean square deviation (RMSD) of impedance as an indicator of damage. Divsholi and Yang [29] provided a method to assess the local and overall damage to a reinforced concrete (RC) beam based on the EMI technique for a single PZT sensor and the wave propagation technique for multiple PZT sensors. Talakokula et al. [30] used PZT sensors to detect the level of carbonation-induced

* Corresponding author.

https://doi.org/10.1016/j.conbuildmat.2020.119307
0950-0618/

rebar corrosion in RC by computing the conductance RMSD. PZT sensors based on the EMI technique were used for corrosion detection in RC structures in previous studies [31,32]. Khante and Gedam [34] measured the conductance and susceptance of a beam by using embedded smart aggregate sensors for damage detection. Dixit and Bhalla [36] employed PZT patches to monitor the accumulated damage in a plain cement concrete subjected to fatigue and impact-type loads.

For conducting SHM by using PZT sensors, except for damage detection, strength monitoring is crucial in civil engineering. The direct compression test is a traditional method used to evaluate the compressive strength of concrete and mortar, and the test is conducted on cylinders or cube specimens. In the past decade, nondestructive active monitoring by using piezoelectric PZT sensors for cementitious materials has been conducted through wave propagation (WP)-based [39–43] and EMI-based monitoring [26,44–51] with strength indicators [43,51]. PZT sensors can be either embedded in or surface bonded onto cementitious material specimens in both monitoring techniques. A PZT patch exhibits the potential capability of strength and hydration monitoring. Although the performance of the EMI technique in terms of repeatability of signatures and performance consistency was slightly inferior to the performance of the WP technique when PZT patches were employed on the surface of a specimen for mortar strength monitoring [42], the EMI technique, in general, has been proven to be useful for strength monitoring of cementitious materials [49].

PZT ceramics and smart aggregates [17] are commonly applied as sensors for real-time SHM in civil infrastructures. However, the PZT sensor is more effective for metals than for concrete [27]. For concrete SHM, Li et al. [52] suggested that the unavoidable mismatch of acoustic impedance and material density between PZT sensors and cementitious materials (host structure) degrades the signal sensitivity and usually causes false alarms during monitoring. Thus, cement-based piezoelectric composites have been developed for SHM [22,52,53]. This development is especially useful for concrete structures and overcomes the matching problem of acoustic impedance and volume compatibility observed for concrete structures since 2002.

Cement-based piezoelectric composites with bar-like PZT inclusions (1–3 type) and with plate-like PZT inclusions (2–2 type) have higher piezoelectric properties than those with randomly oriented PZT particles (0–3 type). Moreover, some 1–3-type and 2–2-type cement-based piezoelectric composites that are used as sensors and actuators have been applied for traffic monitoring and concrete damage detection [54-56]. Xu et al. [55] mentioned that piezoelectric composite sensors are more sensitive to the impedance influence of the coupled structure, although PZT ceramic sensors have more resonant peaks and larger peak values. They concluded that 2–2-type and 1–3-type cement/polymer based piezoelectric composites with the EMI technique can detect the damage of concrete structures.

Many studies [52,57-65] have been conducted to enhance the piezoelectric properties of 0–3-type cement-based piezoelectric composites (termed as piezoelectric cement) comprising piezoelectric particles and a cement matrix because of lower piezoelectricity. Moreover, for piezoelectric cement with 50% PZT, the values of the piezoelectric strain factor d_{33} were achieved to be $\geq$100 pC/N by using the temperature treatment technique [62-65]. Piezoelectric cement with higher piezoelectric properties, such as d_{33} > 70 pC/N, can be commercially used as sensors and actuators to detect and monitor concrete structures. Piezoelectric cement sensors through frequencies, mechanical–electric responses, and AE technologies have been proposed for the use of concrete SHM [66-71]. However, piezoelectric cement sensors based on the EMI technique are still seldom reported for the use of concrete SHM. For the EMI technique, Pan et al. [72] preliminarily employed a piezoelectric cement sensor (0–3 type with 50% PZT) based on the EMI technique to monitor the strength development and to detect damage in concrete. They indicated that the piezoelectric cement sensor can be applied for concrete SHM, and that the electric impedance sensitivity of the piezoelectric cement sensor is higher than that of the PZT sensor when the piezoelectric cement sensor has a d_{33} value of 101 pC/N.

In this study, piezoelectric cement as a sensor embedded in cement mortar was used to evaluate the strength development of the mortar from 1 to 56 days by using the EMI technique. The piezoelectric cement sensor (PEC sensor) comprised PZT ceramic particles and cement in equal volumes, that is, 50% volume of each, and was polarized to induce piezoelectricity. A PZT sensor fabricated using 100% PZT ceramic was used as the counterpart in the experiments. The PEC and PZT sensors were subjected to the same poling process. Three cement mortar types with water-to-cement ratios (w/c) of 0.4, 0.5, and 0.6 were used. Moreover, two sensors—PEC and PZT—were used with the EMI technique and embedded in mortar to assess the compressive strength of the mortar specimens.

2. Experiments

2.1. Manufacturing of piezoelectric specimens

For PZT/cement composites, the composite with 40–50 vol% PZT was found to have an acoustic impedance matching that of concrete [52]. To diminish the mismatch in acoustic impedance and deformation between the PZT sensor and cementitious materials, piezoelectric cement, which is a two-phase PZT/cement composite with PZT particles and type I Portland cement in equal proportions in terms of volume, was used. The acoustic impedance ρ_v of the piezoelectric cement was approximately 9–10 $\times$ 10^6 kg-m^{-2}s^{-1}, which is close to the ρ_v value of concrete (9 $\times$ 10^6 kg-m^{-2}s^{-1}). The cement matrix in this study was fresh cement, and it had a fineness value of 349 m^2/kg and specific gravity of 3.15. Nonpolarized PZT ceramic, which was a flat disk originally, was pulverized to 75–150-μm particles with a specific gravity of 7.9, d_{33} value of 470 pC/N, relative dielectric constant ε_r of 2100, dielectric loss D of 1.5%, and thickness electromechanical coupling coefficient K_t of 0.72; this was provided by Eleceram Technology Co. Ltd., Taiwan.

To fabricate the piezoelectric cement specimen (PEC specimen), PZT particles and cement were mixed uniformly by using a solar-planetary mill for 5 min without adding water. Then, the mixture (composite) was placed in a cylindrical steel mold with a diameter of 15 mm and pressed by applying 80 MPa compression. Thus, a disk-like specimen was formed. The specimens were cured at 90 °C and a relative humidity of 100% for 24 h to produce suitable strength. After curing, the specimens were polished to a thickness of 2 mm. Both sides of the specimens were coated with silver paste (SYP-4570, Ag PRO Technology Corp.) to form the electrodes. A PZT ceramic specimen in the shape of a flat disk with 12-mm diameter and 1.8-mm thickness was provided by a commercial company, and the properties of the specimen are the same as the PZT particles in piezoelectric cement.

Prior to polarization, the PEC specimen was subjected to the pretreatment and post-treatment at 140 °C for 40 min [64]. The temperature treatment technique involves double heating on the specimen before and after the manufacturing of electrodes. However, the PZT specimen did not undergo the double-heating process in this study because the heating temperature has less influence on the d_{33} value of PZT ceramic [62]. Both the PEC and PZT specimens

were polarized by applying 1.5 kV/mm at 150 °C for 40 min to induce piezoelectricity.

2.2. Properties of piezoelectric specimens

After completion of polarization, the piezoelectric properties of the piezoelectric specimens were measured at 23 °C and a relative humidity of 50% for 100 days. Fig. 1 displays the d_{33} values of the PZT and PEC specimens, where each experimental value is an average of nine positions of the specimens and the solid lines are the average of three specimens. The d_{33} values of the PZT specimens were not sensitive to their age, and the average value was approximately 422 pC/N. However, the d_{33} values of the PEC specimens depended on specimen age and approached a constant value (d_{33} = 99 pC/N) after 70 days. Previous studies [58,73,74] indicated that the d_{33} values developed with the age and gradually reached constant are always observed from 10 to 60 days after the polarization, depending on PZT content and size, specimen forming technique, poling time and applying voltages. The mechanisms of age-dependent d_{33} for 0–3 type PZT/cement composites are still under investigated. Pore structures and the main hydrated products (CH and CSH) in cement matrix are influence factors on the development of d_{33} with age. As the age increases, less pores were found in the specimen, resulting in higher intensity of stress transmission which enhances d_{33}. In essence, the d_{33} value of the PZT specimens is higher than of the PEC specimens.

Fig. 2 and Fig. 3 display the impedance Z of the PZT and PEC specimens from the first day to the 90th day after polarization. The electrical impedance decreased with the increase in the scan frequency for both the PZT and PEC specimens, except at the resonant frequency. Moreover, the impedance value of the PZT specimen in Fig. 2 had no age dependence; that is, the impedance on the 90th day was almost the same as that on the first day. However, the electrical impedance of the PEC specimen in Fig. 3 declined rapidly during the first 7 days and then gradually approached asymptotic stability after 60 days, that is, the impedance of the PEC specimen underwent less change after 60 days. The PEC specimen after 60 days is the timing to fabricate PEC sensor. Noted that the electrical impedance decreased with the age of the PEC specimen that was not equivalent to the reduction in the resistance (R) of the PEC specimen. The experimental data indicated that the resistance, which is the real component of the electrical impedance, of the PEC continued to increase with age.

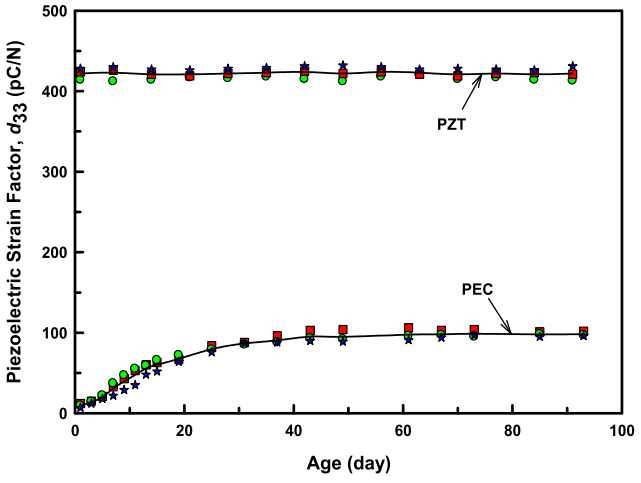

Fig. 1. Piezoelectric strain factor d_{33} of PZT and PEC specimens.

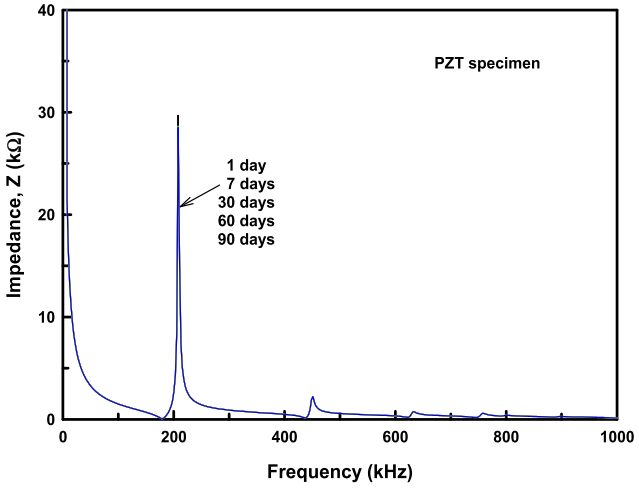

Fig. 2. Impedance spectra of the PZT specimen for 90 days.

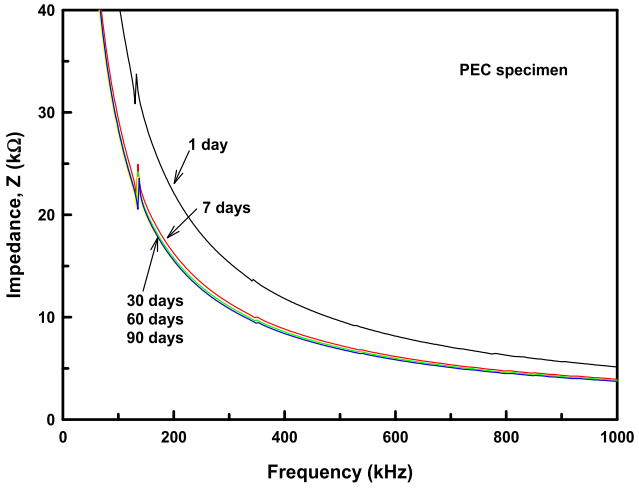

Fig. 3. Impedance spectra of the PEC specimen for 90 days.

2.3. Mortar specimens and sensor packaging

Cement mortar comprised type I Portland cement and the ASTM C778 standard sand with the mass proportion of cement to sand of 1:2.75 in all the mortar mixes. The mortar specimen was a 50-mm cube. The compressive strength of three cement mortar types with different w/c ratios of 0.4, 0.5, and 0.6 was evaluated at the specimen ages of 1, 3, 7, 14, 21, 28, and 56 days by conducting the direct compressive test.

The piezoelectric sensors were fabricated using the PZT and PEC specimens as sensing elements and asphalt as the packaging material. The asphalt coating (packaging material) entirely covered the sensing element (circular disk) and copper foil tape (as conductive wires) to ensure sufficient insulation ability of the sensor, as shown in Fig. 4. Then, heat-shrinkable tubing (thermal casing) was wrapped on the sensor, except for the sensing element part, to ensure the insulation protection of conductive wires. To evaluate the strength development in mortar, a piezoelectric sensor was embedded in the center of each mortar specimen that underwent wet curing, as shown in Fig. 5. Moreover, the impedance spectra corresponding to the age of the specimen under direct compressive testing were obtained for 56 days.

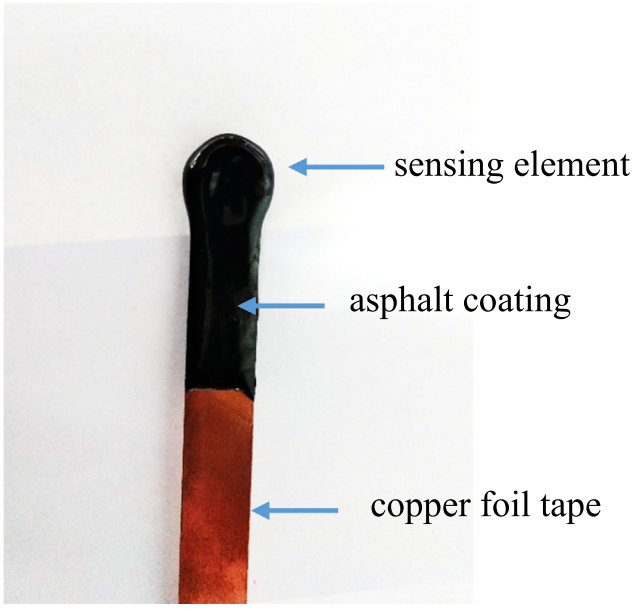

Fig. 4. Compositions of the piezoelectric sensor.

Fig. 5. Mortar specimens with embedded piezoelectric sensors cured in water.

2.4. EMI measurement

The piezoelectric PEC and PZT sensors serve as piezo-impedance sensors embedded in cement mortar (the host structure). The EMI technique is based on dynamic equilibrium of dynamic sensor properties and structural stiffness. The electrical admittance $\bar{Y}$ (the reciprocal of impedance) of the piezoelectric material is governed by the following equation [75]:

$$\bar{Y} = G + iB = 4\omega i \frac{l^2}{h}\left[\overline{\varepsilon_{33}^T} - \frac{2d_{31}^2\overline{Y^E}}{(1-\nu)} + \frac{2d_{31}^2\overline{Y^E}}{(1-\nu)}\left(\frac{Z_{a,eff}}{Z_{s,\text{eff}}+Z_{a,\text{eff}}}\right)\overline{T}\right] \quad (1)$$

where G represents conductance, B represents susceptance, i is the imaginary unit, and w is the circular frequency of the electric field applied for actuation. Moreover, l and h are the half-length and thickness values of the piezoelectric material (sensor), respectively. $\overline{\varepsilon_{33}^T}$ is a complex dielectric constant at a constant stress, d_{31} is the piezoelectric strain factor, $\overline{Y^E}$ is the complex Young's modulus under a constant electric field, ν is the Poisson's ratio of piezoelectric material, and $\overline{T}$ is the complex tangent ratio. Here, $Z_{a,\text{eff}}$ and $Z_{s,\text{eff}}$ are the mechanical impedance of the piezoelectric material and the substrate (the host structure), respectively. In Eq. (1), as the impedance of the host structure $Z_{s,\text{eff}}$ changes, the electrical admittance $\bar{Y}$ also varies. That is, any change in the mechanical properties of the host structure causes changes in the mechanical impedance that induces changes in the electrical impedance of the piezoelectric sensor [23,25]. This provides the basis for the sensing methodology for inferring the mechanical impedance of the surrounding structure. In monitoring, the magnitude of the admittance value is not the main concern, but the change of admittance. Therefore, when the sensor is embedded in the mortar in different orientations, the directivity of sensor has little effect on the strength monitoring results. Moreover, Park et al. [24] indicated that the imaginary component of the electrical admittance (or susceptance B) is more sensitive to temperature variation than the real component (conductance). This implies that conductance G is more preferable for SHM. This well-known EMI technique using PZT patches and smart aggregates has been applied for monitoring the strength development of cementitious materials [44-51].

Here, a PEC sensor embedded in cement mortar was used to evaluate the mortar strength by using the EMI technique. The electric impedance spectra of the sensor were acquired using an impedance analyzer (Wayne Kerr 6520A) in the scan range of 20–2000 kHz with 1600 points, as shown in Fig. 6. Each impedance value that was obtained at an interval of 1.25 kHz. A specific frequency range was selected as the effective monitoring frequency. In this range, the conductance decreased with increasing age. Conductance changes in this frequency range was used to calculate the RMSD. The conductance RMSD is as indicator, and it correlated with the specimen strength development.

3. Results and discussion

3.1. Impedance of piezoelectric sensor

After the polarization of the PZT and PEC specimens, the electric impedance on the 90th day (piezoelectric specimen), 91st day (specimen adhered with copper foil tape), 92nd day (specimen after the asphalt coating), and 93rd day (the sensor embedded in the mortar) was compared, as shown in Figs. 7 and 8. The impe-

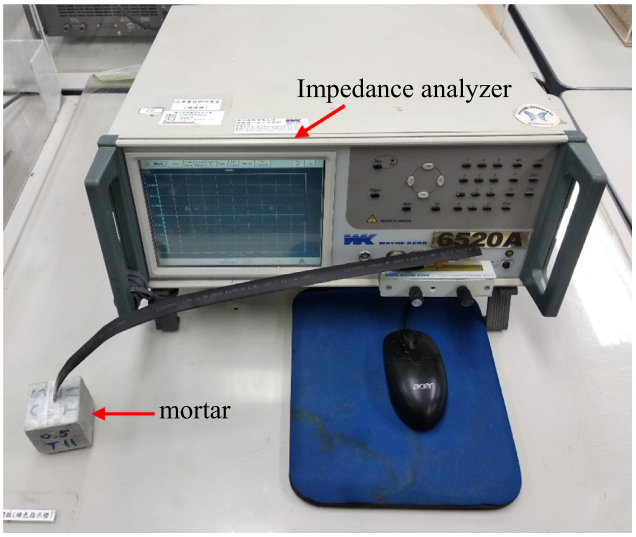

Fig. 6. Electrical impedance measurement of cement mortar.

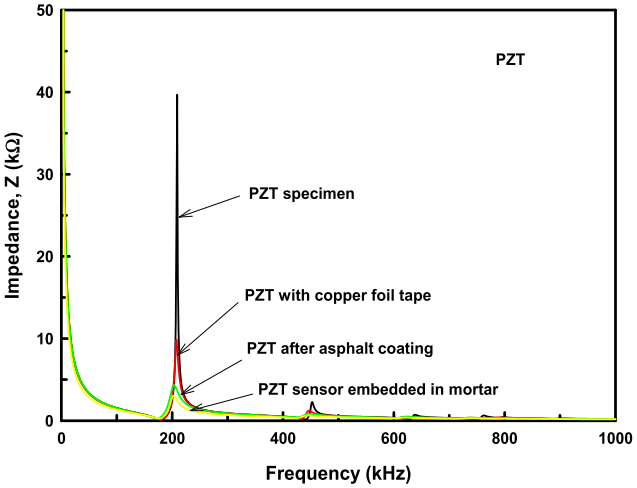

Fig. 7. Impedance spectra of the PZT specimen before and after packaging.

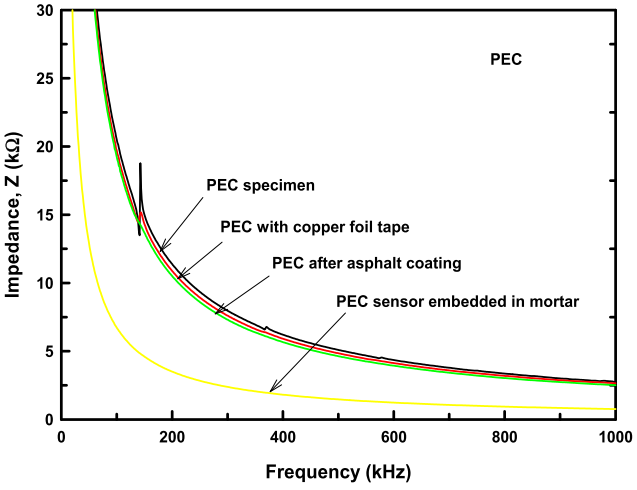

Fig. 8. Impedance spectra of the PEC specimen before and after packaging.

dance spectra of the PZT specimen before and after packaging are shown in Fig. 7. An apparent resonant frequency was observed near 200 kHz (the first resonant peak) prior to the packaging of the PZT specimen. After the copper foil tape was affixed to the electrodes using silver paste (SYP-70A), the impedance at the resonant peak of the specimen considerably decreased from approximately 40 kΩ to 10 kΩ. The resonant peak continued to decline after the asphalt coating. Then, the resonant peak for the PZT sensor embedded in the mortar was found to be the lowest. The packaging of the PZT specimen caused a decline of the conductance in the resonant peaks because the surrounding materials (copper foil tape, asphalt, and mortar) affected the electrical impedance of the PZT sensor, as verified using Eq. (1). Similar investigations on the conductance of the PZT patch attached on the surface of the concrete specimens [45] and embedded inside the mortar specimens [76] were also reported. The first resonant peak of the PZT sensor was still visualized after the PZT sensor was embedded in the mortar specimens, although the resonant peaks exhibited a large decline. Compared with the PZT specimen (without the packaging materials), the impedance decrease of the embedded PZT sensor was very small in the scan frequency range of 20 Hz – 1000 kHz, except for the impedance near the resonant peaks.

It is necessary to pack the PEC specimen after 60 days of polarization due to the age-dependent impedance (Fig. 3). In this study, PEC packaging was conducted after 90 days. Fig. 8 displays the impedance spectra of the PEC specimen before and after packaging. The primary resonant peaks (near 150 kHz) decreased when the PEC specimen was covered with asphalt, similar to the finding for the PZT sensor. However, the impedance value declined apparently in the entire scan frequency and in the absence of a resonant peak when the PEC sensor was embedded in mortar (cementitious material). This distinct impedance change indicates that the PEC sensor is more suitable for cementitious material SHM than the PZT sensor because of its impedance sensitivity in mortar.

3.2. Conductance and the age

Twelve specimens were prepared for each mortar type. A piezoelectric sensor comprising six PZT and six PEC sensors was embedded in each specimen to measure the conductance values for 56 days. Fig. 9 displays the conductance spectra of the PZT-1 sensor in the mortar specimen with a w/c ratio of 0.5 from day 0 to day 56, where day 0 represents the final setting time of the mortar. The first peak of the conductance spectra is in the range of about 50–150 kHz. Within this range, the conductance spectra oscillate extraordinarily and no regular trends in conductance change with the age were observed, leading to find an effective monitoring frequency range difficultly. The conductance near the second resonant peak (zone A, 334–364 kHz) and the third resonant peak (zone B, 496–561 kHz) exhibited a declining trend with the increase in specimen age. These two frequency zones are the effective monitoring frequencies of the PZT-1 sensor that are suitable for the strength monitoring of mortar because the conductance decreases with increase in the age, thus reflecting that some physical meanings that correlate with the mortar strength and specimen age. Table 1 lists the effective monitoring frequencies of the six embedded PZT sensors for each mortar. The effective frequencies of all three mortar types were at the second resonant peak but were not always observed at the third peak.

The conductance spectra of the embedded PEC sensors in the mortar specimen were also acquired for 56 days. For example, the conductance spectra of the PEC-1 sensor at a w/c ratio of 0.5 is shown in Fig. 10. No resonant peaks were observed. Moreover, the conductance curves of the PEC-1 sensor exhibited less fluctuation in the entire scan frequency compared with the PZT-1 sensor in Fig. 9. The conductance curves displayed in Fig. 10 are smooth. Thus, the conductance changes can be more effectively distinguished with the increase in age. In other words, the regularity between the conductance and specimen age can be easily recognized in the conductance curves measured using PEC sensors. The conductance variations increased as the frequency increased.

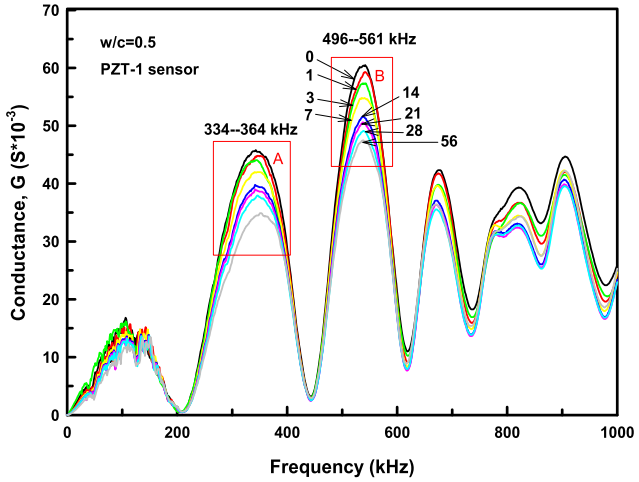

Fig. 9. Conductance spectra of the PZT-1 sensor in the mortar for 56 days.

Table 1
Effective monitoring frequency of embedded PZT sensors in mortar.

Mortar		Effective monitoring frequency (kHz)					
		PZT-1	PZT-2	PZT-3	PZT-4	PZT-5	PZT-6
w/c = 0.4	2nd peak	330–368	347–385	311–382	325–375	279–371	334–342
	3rd peak	520–557	534–561	—*	501–557	496–576	519–556
w/c = 0.5	2nd peak	334–364	268–334	275–350	332–388	260–345	315–370
	3rd peak	496–561	517–588	505–554	—*	484–571	—*
w/c = 0.6	2nd peak	309–364	283–358	297–364	274–361	274–388	325–343
	3rd peak	510–590	—*	—*	—*	511–559	514–543

* Note: Conductance has no sequent order pertaining to the ages.

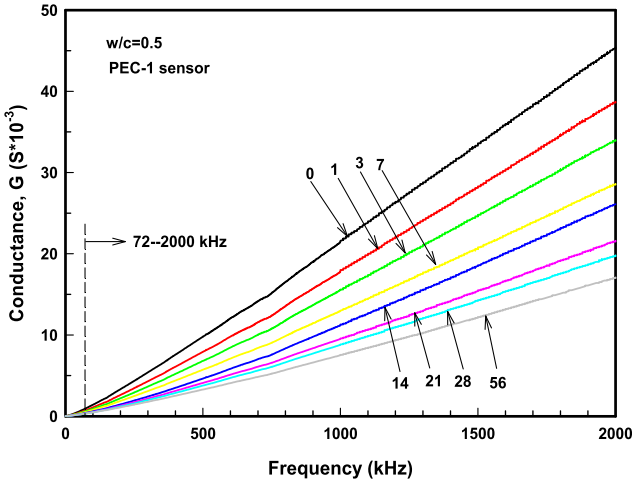

Fig. 10. Conductance spectra of the PEC-1 sensor in the mortar for 56 days.

Moreover, the effective monitoring frequency of the PEC-1 sensor in the mortar specimen with a w/c ratio of 0.5 was 72–2000 kHz. Within effective monitoring frequencies, the conductance decreased (or the resistance increased) with the increase in mortar specimen age, thus reflecting a connection between mortar strength and specimen age. Table 2 lists the effective monitoring frequency of six embedded PEC sensors in each mortar. A comparison of Table 1 and Table 2 reveals that the bandwidth of the effective monitoring frequency of the PEC sensor is broader than the bandwidth of the PZT sensor. The reason for the broader bandwidth is that the mechanical properties and acoustic impedance of the PEC sensor, fabricated by PEC which is a piezoelectric composite, are much close to those of cement mortar. Thus, compared with the PZT sensor, the PEC sensor is more sensitive to conductance variations as the mortar conductance changes. This superior monitoring characteristic makes the PEC sensor more applicable to cementitious material SHM.

3.3. Conductance and compressive strength

For PZT sensors, two methods can be used to assess the strength development and mechanical properties of cementitious materials: using frequency peak and using conductance at the resonant peak [26,42,44-51,55,76,77]. Here, the conductance at the resonant peak of the embedded PZT was selected to correlate with the mortar strength. Fig. 11 displays the conductance of the embedded PZT-1 sensor at two resonant peaks (348 kHz at the second peak and 541 kHz at the third peak in Fig. 9) in a mortar specimen with a w/c ratio of 0.5. The two conductance curves display the trend of decrease in conductance with the increase in the mortar age. This result is observed because more hydration of the mortar induces more cement solids, which increase the electric resistance of mortar. In other words, an increase in the compressive strength with age causes a conductance decrease. The conductance–age curves of other PZT sensors, with conductance values at 28 resonant peaks within the effective monitoring frequency presented in Table 1, have similar conductance decreases with the ages. The conductance at the resonant peak is correlated with the strength development if the PZT sensor is applied. Obviously, the conductance selected at the second resonant peak by the PZT measurement is valid and reliable for mortar strength monitoring because the effective monitoring frequency always occurs near the second resonant peak, as listed in Table 1.

Fig. 12 shows the conductance of the specimen at a w/c ratio of 0.5 that was measured using the PEC-1 sensor at 500 kHz and 1800 kHz, where 500 kHz and 1800 kHz were picked arbitrary within the effective frequency range (Fig. 10). The conductance curves display a decreasing trend as the compressive strength of the mortar specimen increases. This correlation between the conductance and strength was found for all conductance values at the specific frequency within the effective monitoring frequency range (72–2000 kHz) in Fig. 10. This decreasing trend of conductance with the increase in strength is also true for the conductance selected at any frequency within the effective monitoring frequency in Table 2. This means that the conductance corresponding to a frequency within the effective monitoring frequency range has the capability of mortar strength monitoring if the PEC sensor is used. Compared with the PZT sensor, the PEC sensor has the advantage of a broader effective frequency for mortar strength monitoring. Thus, the PEC sensor is a conducive replacement to the PZT, especially for cementitious material SHM.

3.4. Conductance RMSD and compressive strength

Many parameters, such as RMSD, mean absolute percentage derivation (MAPD), and correlation coefficient derivation (CCD),

Table 2
Effective monitoring frequency of embedded PEC sensors in mortar.

Mortar	Effective monitoring frequency (kHz)					
	PEC-1	PEC-2	PEC-3	PEC-4	PEC-5	PEC-6
w/c = 0.4	594–2000	383–2000	57–2000	84–2000	853–2000	—*
w/c = 0.5	72–2000	783–2000	434–2000	330–2000	392–2000	423–2000
w/c = 0.6	801–2000	167–2000	251–2000	49–2000	1163–2000	134–2000

* Note: Conductance in some discrete frequency ranges has sequent order pertaining to the ages.

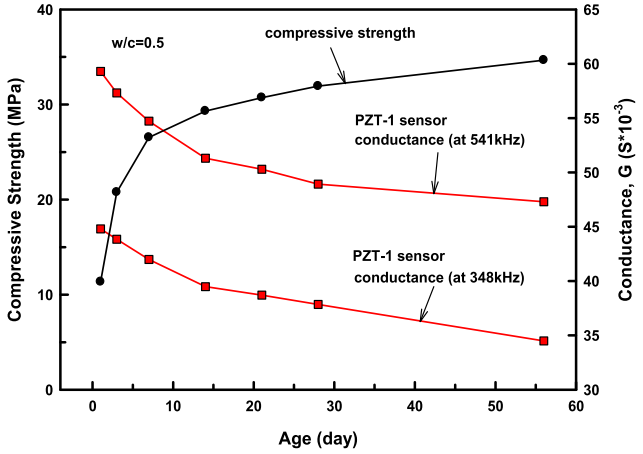

Fig. 11. Conductance of the PZT-1 sensor at the resonance peak correlated with compressive strength.

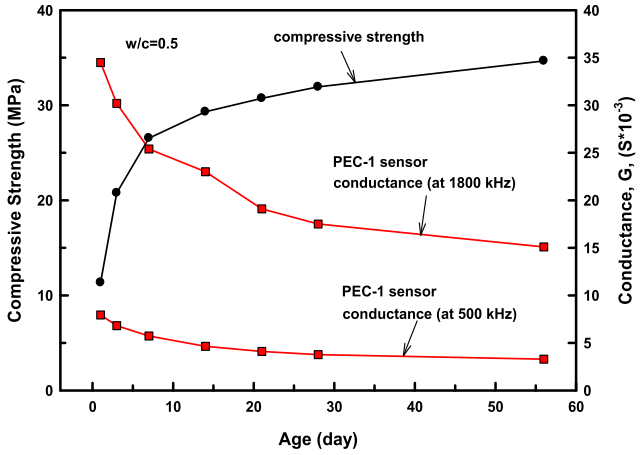

Fig. 12. Conductance of the PEC-1 sensor at a specific frequency within the effective frequency correlated with compressive strength.

have been employed to correlate the strength development of cementitious materials with the electrical conductance of PZT sensors [26,46,50,51]. RMSD was suggested to be the most accurate parameter among all parameters for monitoring the properties of cementitious materials at an early age [51]. Wang and Zhu [46] suggested that the RMSD of real admittance (conductance) provides a more accurate reflection the variations in concrete compressive strength than the RMSD of imaginary admittance (susceptance) if the PZT patch was embedded in a concrete cube for 28 days. Here, the RMSD index of conductance was used to evaluate the compressive strength of cement mortar.

Fig. 13 displays the actual correlation between the compressive strength and the conductance RMSD of the PZT-1 sensor that was placed in the mortar specimen with a w/c ratio of 0.5 at different ages, where the baseline spectra at the final setting time (day 0) of the mortar were chosen to calculate the RMSD at different ages of the mortar specimen. The conductance values that were obtained at an interval of 1.25 kHz were selected within the effective monitoring frequency of the second and third peaks (Fig. 9). The regression curves of the conductance RMSD and the age in Fig. 13 satisfy a two-parameter logarithmic behavior expressed as follows.

$$G_R = a_1 + a_2 \ln t \tag{2}$$

where G_R is the RMSD value of conductance, t represents the age (unit: day), and a_1 and a_2 are the material parameters. This relation

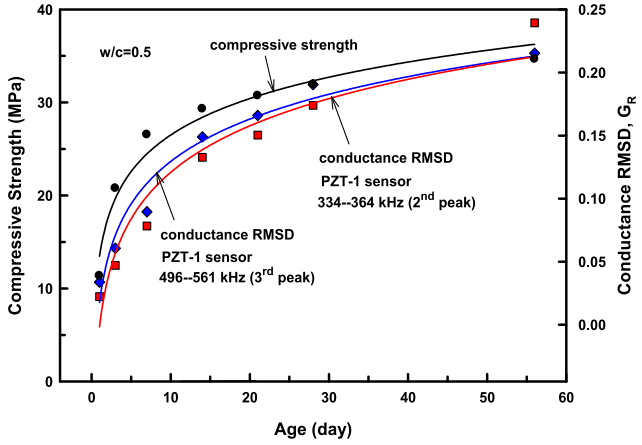

Fig. 13. The development trends between the compressive strength at a w/c ratio of 0.5 and conductance RMSD of the PZT-1 sensor near the resonant peaks.

is also suitable for the other PZT sensors embedded in mortar if the conductance RMSD was calculated within the effective monitoring frequency range. Moreover, the regression curve pertaining to the experimental compressive strength f_c of the mortar specimens at different ages (in Fig. 13) also presents a logarithmic function as that presented in Eq. (2) and has the following form:

$$f_c = a_3 + a_4 \ln t \tag{3}$$

where a_3 and a_4 are the material parameters. This logarithmic relation is similar to an exponent function proposed by Wang and Zhu [46] for a concrete specimen at the age of 1–28 days and can be given as follows:

$$y = \exp[b_1 + b_2/(x + b_3)] \tag{4}$$

where y is the compressive strength of the concrete specimen, x is the age of the specimen, and b_1, b_2, and b_3 are the material parameters. Fig. 13 reveals that the compressive strength f_c has a strong high correlation with G_R at different ages.

However, this high correlation for all mortars monitored using the PZT sensors was obtained only for the conductance RMSD calculated from the effective monitoring frequency near the second peak because some RMSDs calculated from the conductance near the third peak (Table 1) did not always exhibit regularity with increase in the age of the specimen. Due to some uncertain risks of finding the effective monitoring frequency near the third peak and to ensure the reliability of mortar compressive strength estimation, the conductance near the second peak was suitable to calculate the RMSD value if the PZT sensor was used.

When the PEC sensor was embedded in the mortar, the experimental compressive strengths and two conductance RMSD curves were determined for the specimens with w/c ratios of 0.4, 0.5, and 0.6 (Figs. 14–16). In this case, the RMSD values were calculated corresponding to their effective monitoring frequency in Table 2. All regression curves of the conductance RMSD measured using the PEC sensor also followed a logarithmic behavior in Eq. (2) when the coefficient of determination r^2 was >0.97. The development trends between the compressive strength and the conductance RMSD with the ages were very similar to each other. After inspecting the conductance signatures of all PEC sensors within the effective monitoring frequency (Table 2), all PEC sensors were found to display a similar logarithmic relation related to f_c and G_R at different ages, as expressed in Eqs. (2) and (3). For conducting strength monitoring by using a PEC sensor, the conductance value can be selected at any frequency intervals within the effective frequency range to calculate the RMSD. This result is different from PZT measurement, which only provides a reliable frequency range near the

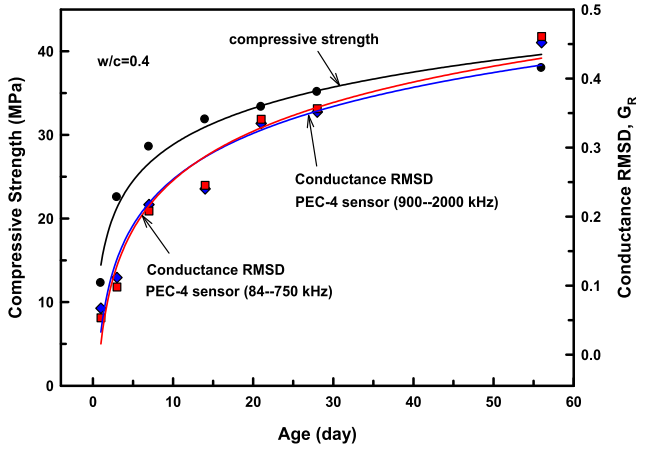

Fig. 14. The development trends between the compressive strength at a w/c ratio of 0.4 and the conductance RMSD of the PEC-4 sensor within the effective frequency.

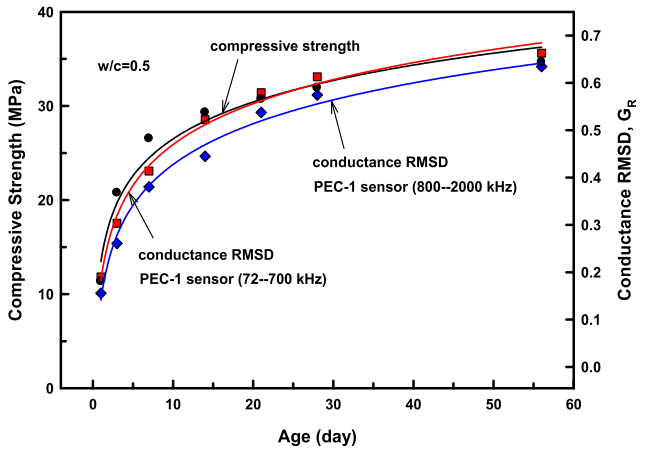

Fig. 15. The development trends between the compressive strength at a w/c ratio of 0.5 and conductance RMSD of the PEC-1 sensor within the effective frequency.

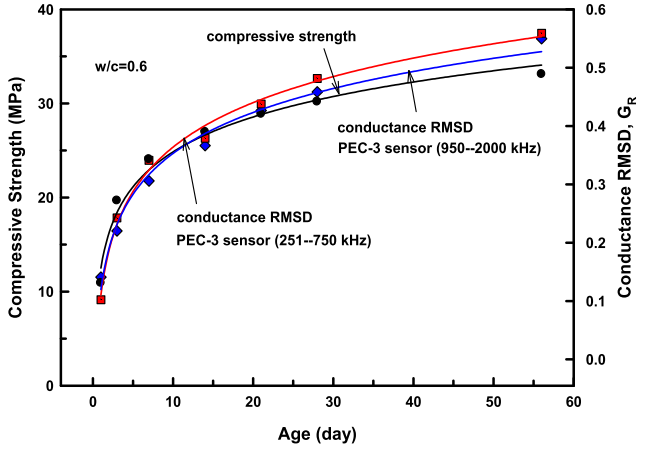

Fig. 16. The development trends between the compressive strength at a w/c ratio of 0.6 and conductance RMSD of the PEC-3 sensor within the effective frequency.

second peak. Moreover, the RMSD ranges presented in Figs. 14-16 exhibit bigger than the ranges measured using the PZT sensor (Fig. 13). For instance, at w/c = 0.5 the G_R range in Fig. 15 (PEC sensor) is 0.75, greater than that 0.25 in Fig. 13 (PZT sensor). This implies that the PEC sensor has higher the sensitivity for strength monitoring of cementitious materials than the PZT sensor.

3.5. Determination of compressive strength

To assess the compressive strength of mortar by using an embedded piezoelectric sensor and the EMI technique, the correlations between the compressive strengths of the mortar specimen and conductance RMSD values using the PZT and PEC sensor were considered and are plotted in Figs. 17 and 18, respectively, for different w/c ratios. The regression curves related to the compressive strength and conductance RMSD for both piezoelectric sensors exhibit nonlinear relation and satisfy the following equation:

$$f_c = c_1 + c_2 \ln(G_R - c_3) \tag{5}$$

where f_c is the compressive strength and c_1, c_2, and c_3 are the material parameters. The relation between compressive strength and EMI-based-conductance RMSD is a three-parameter logarithmic function for PZT sensors in Fig. 17 with $r^2 > 0.94$ and for PEC sensors in Fig. 18 with $r^2 > 0.97$. This logarithmic relationship presented in Eq. (5) is valid for the compressive strength of the mortar specimens monitored through PZT and PEC measurements.

A similar study on the concrete strength monitored by the PZT sensor for 28 days revealed an exponential relation between the strength and RMSD values [46]. In this case, the RMSD value was calculated from the conductance in the range of 150–350 kHz near resonant peak. The RMSD calculations in the selected frequency range [46] did not full consider whether the decrease in the conductance is related to the increase in concrete age. Thus, the curves between the compressive strength and the conductance RMSD exhibited an upward trend as the conductance RMSD increased (that is, the concrete compressive strength tended toward infinity as the RMSD values increased). In Figs. 17 and 18, the conductance RMSD values were calculated by considering the conductance within the effective monitoring frequency. The results revealed that a logarithmic relation is obtained between f_c and G_R, that is, the compressive strength tended toward finite values if the conductance RMSD continued to increase. The construction of the f_c–G_R curve with a logarithmic relation in Eq. (5) seems more reasonable for mortar. Moreover, Su et al. [51] investigated early age (4 h to seventh day) strength of the mortar specimens by using PZT patches mounted on the surface of the specimens and found a linear correlation between the strength at an early age and RMSD indices, where the conductance RMSD were processed at the frequency range from 100 k to 400 kHz. This approximate correlation is somehow obtained in Fig. 17 and Fig. 18 at the first three points (first, third, and seventh day) of the f_c–G_R curves. The electrical conductance obtained in the effective monitoring frequency range

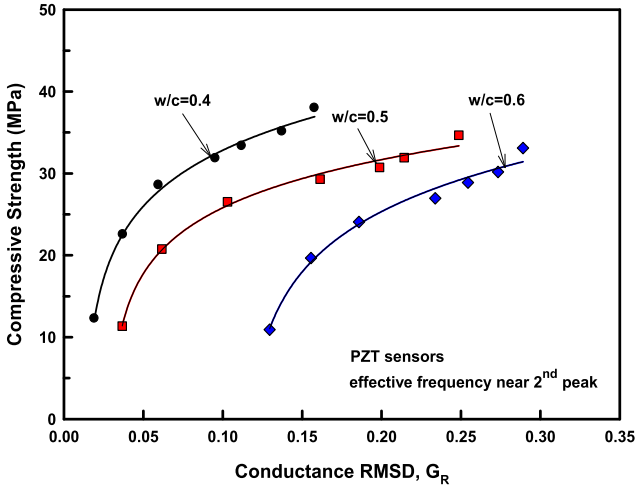

Fig. 17. Relation of conductance RMSD of the PZT sensor and compressive strength.

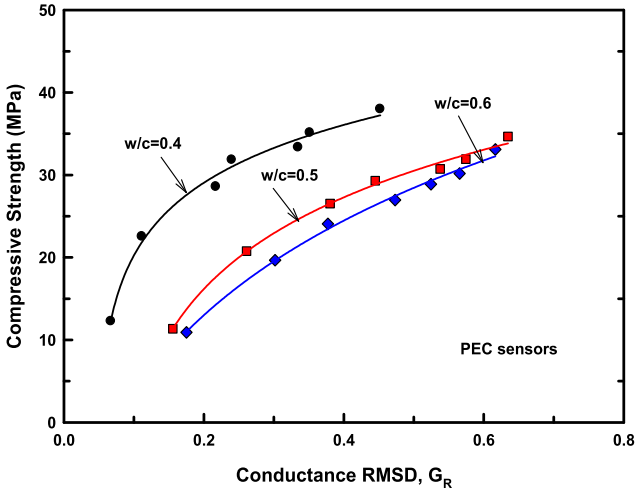

Fig. 18. Relation of conductance RMSD of the PEC sensor and compressive strength.

is necessary to evaluate the compressive strength of cementitious materials if piezoelectric sensors are used for monitoring of cementitious materials based on the EMI technique.

Figs. 17 and 18 show that both the PEC and PZT sensors have similar ability to monitor the compressive strength of mortar. The correlation between conductance RMSD and compressive strength of mortar follows a logarithmic relation, as presented in Eq. (5). In particular, a comparison of Figs. 9 and 10 reveals that the effective monitoring frequency can be selected more conveniently when the PEC sensor is used for mortar (cementitious material) monitoring. Moreover, a comparison of Fig. 13 and Fig. 14 – 16 suggests that the $G_R$sensitivity to assess the compressive strength of mortar is higher when the PEC sensor is used. If a PEC sensor is embedded in mortar to evaluate the compressive strength, conductance signatures used to calculate G_R are suggested to be in the higher frequency range, such as 800–2000 kHz (Table 2). This is based on the observation that a higher frequency range of PEC sensor is easy to fall in the range of effective monitoring frequency, causing more reliable strength determination.

In addition, Figs. 17 and 18 also show that the relationship between the compressive strength and the conductance RMSD is highly dependent on the w/c, because cement mortars (cementitious material) with the same composition but different w/c usually have different compressive strength. The w/c in the mortar can affect the amount and size of pores, the material properties of the cement solids and the solid microstructure of the mortar, and these factors are considered to affect the compressive strength. Similar to the compressive strength, these factors in cement mortar also affect the conductance. Even cement mortars with the same compressive strength may have different conductance and vice versa. For instance, given a conductance RMSD of 0.15 from PZT sensor (Fig. 17), the predicted compressive strength could vary from 20 MPa to about 40 MPa (100% difference). Similarly, given a conductance RMSD of 0.3 measured from PEC sensor (Fig. 18), the predicted compressive strength value could change from 20 MPa to 30 MPa (50% of difference). Obviously, it is difficult to predict compressive strength using only a single measurement parameter (such as electric conductance or frequency), just as other NDT methods may encounter similar difficulties in SHM. Therefore, it is necessary to establish a specific database corresponding to its NDT technology and the measured object, especially for commercial use. Here, when considering the w/c effect, it is suggested to use the power law to modify the relationship between the compressive strength and conductance RMSD in Eq. (5), that is, the modified equation has the form of $f_c = [c_1 + c_2 \ln(G_R - c_3)] \cdot p(w/c)$, where the factor p(w/c) affected by the w/c can be determined from experiments and regression analysis. Once the $p(w/c)$ is known, the compressive strength of cement mortar can be estimated from the G_R. The more influence factors considered, the more accurate the prediction of compressive strength.

4. Conclusions

The PEC sensor fabricated by mixing 50% PZT particles in cement matrix had an acoustic impedance close to that of concrete prepared for SHM. A PEC sensor with a d_{33} value of 99 pC/N was embedded in a mortar specimen to evaluate the compressive strength for 56 days. The PEC sensor based on the EMI technique was investigated and compared with a PZT sensor. The experiments revealed that, compared with the PZT sensor, a more sensitive distinction was observed in the electrical impedance of the PEC sensor before and after the sensor was embedded in mortar. This implies that the PEC sensor is superior to the PZT sensor for strength monitoring for cementitious materials. The PEC sensor is beneficial for evaluating the change in the material properties in SHM with higher accuracy. According to the trend of conductance decrease with specimen age, the conductance in the effective monitoring frequency was selected to calculate the RMSD correlated with the strength. For mortar strength monitoring by using the PZT sensor, the effective monitoring frequency was usually present near the second resonant peak with a narrow frequency bandwidth of less than 100 kHz. For most embedded PEC sensors, the effective monitoring frequency located at the higher frequency region can be selected, that is, 800–2000 kHz in this study, to ensure reliable strength estimation of the mortar. This causes the effective monitoring frequency of PEC sensor more easily to be obtained than that of the PZT sensor during cementitious material SHM. Based on the conductance RMSD in the effective monitoring frequency, the relation between the mortar compressive strength and the conductance RMSD was concluded to have a three-parameter logarithmic function shown in Eq. (5). The logarithmic relation of f_c and G_R was valid from day 1 to day 56 for the cement mortar monitored using the PZT and PEC sensors. The PEC sensor can be used as a replacement of the PZT sensor, especially for the SHM of cementitious materials.

Author Contribution Statement

The corresponding author is responsible for ensuring that the descriptions are accurate and agreed by all authors.

Declaration of Competing Interest

The authors declare that they have no known competing financial interests or personal relationships that could have appeared to influence the work reported in this paper.

Acknowledgments

This work was supported by the Ministry of Science and Technology of Taiwan (MOST 107-2221-E-992-037).

References

[1] ACI Committee 228. In-place methods to estimate concrete strength, Report 228.IR-03, Farmington Hills, MI: American Concrete Institute (2003).
[2] S.W. Shin, A.R. Qureshi, J.Y. Lee, C.B. Yun, Piezoelectric sensor based nondestructive monitoring of strength gain in concrete, Smart Mater. Struct. 17 (2008) 055002.
[3] S.P. Pessiki, N.J. Carino, Setting time and strength of concrete using the impact-echo method, ACI Mater. J. 85 (1988) 389–399.

[4] G.F. Kheder, A.M. Al Gabban, S.M. Abid, Mathematical model for the prediction of cement compressive strength at the ages of 7 and 28 days within 24 hours, Mater. Struct. 36 (2003) 693–701.
[5] T. Ozturk, O. Kroggel, P. Grubl, J.S. Popovics, Improved ultrasonic wave reflection technique to monitor the setting of cement-based materials, NDT & E Int. 39 (2006) 258–263.
[6] Y. Lu, J. Li, L. Ye, D. Eang, Guided wave for damage detection in rebar-reinforced concrete beams, Constr. Build. Mater. 47 (2013) 370–378.
[7] P. Antunes, H. Lima, H. Varum, P. Andre, Optical fiber sensors for static and dynamic health monitoring of civil engineering infrastructures: abode wall case study, Measurement 45 (2012) 1695–1705.
[8] D. Yang, J. Wang, D. Li, K.S.C. Kuang, Fatigue crack monitoring using plastic optical fibre sensor, Procedia Struct. Integ. 5 (2017) 1168–1175.
[9] F.J. Baeza, O. Galao, E. Zornoza, P. Garces, Multifunctional Cement Composites Strain and Damage Sensors Applied on Reinforced Concrete (RC) Structural Elements, Materials 6 (2013) 841–855.
[10] E. Verstrynge, H. Pfeiffer, M. Wevers, A novel technique for acoustic emission monitoring in civil structures with global fiber optic sensors, Smart Mater. Struct. 23 (2014) 065022.
[11] W. Li, Q. Kong, S.C.M. Ho, I. Lim, Y.L. Mo, G. Song, Feasibility study of using smart aggregates as embedded acoustic emission sensors for health monitoring of concrete structures, Smart Mater. Struct. 25 (2016) 115031.
[12] W.Y. He, W.X. Ren, Structural damage detection using a parked vehicle induced frequency variation, Eng. Struct. 170 (2018) 34–41.
[13] F. Frigui, J.P. Faye, C. Martin, O. Dalverny, F. Oeres, S. Judenherc, Global methodology for damage detection and localization in civil engineering structures, Eng. Struct. 171 (2018) 686–695.
[14] M.K. Moradllo, Q. Hu, M.T. Ley, Using X-ray imaging to investigate in-situ ion diffusion in cementitious materials, Constr. Build. Mater. 136 (2017) 88–98.
[15] T. Suzuki, T. Shiotani, M. Ohtsu, Evaluation of cracking damage in freeze-thawed concrete using acoustic emission and X-ray CT image, Constr. Build. Mater. 136 (2017) 619–626.
[16] A. Davis, M. Mirsayar, D. Hartl, Structural health monitoring using embedded magnetic shape memory alloys for magnetic sensing, Proc. SPIE 10971 (2019) 109710O.
[17] G. Song, H. Gu, Y.L. Mo, Smart aggregates: multi-functional sensors for concrete structures—a tutorial and a review, Smart Mater. Struct. 17 (2008) 033001.
[18] P.W. Chen, D.D.L. Chung, Concrete as a new strain/stress sensor, Compos. Part B 27B (1996) 11–23.
[19] S. Wen, S. Wang, D.D.L. Chung, Piezoresistivity in continuous carbon fiber polymer– matrix and cement–matrix composites, J. Mater. Sci. 35 (2000) 3669–3675.
[20] M. Sun, Q. Liu, Z. Li, Y. Hu, A study of piezoelectric properties of carbon fiber reinforced concrete and plain cement paste during dynamic loading, Cem. Concr. Res. 30 (2000) 1593–1595.
[21] H. Zhang, S. Hou, J. Ou, Smart aggregates for monitoring stress in structural lightweight concrete, Measurement 122 (2018) 257–263.
[22] S. Wen, D.D.L. Chung, Cement-based materials for stress sensing by dielectric measurement, Cem. Concr. Res. 32 (2002) 1429–1433.
[23] C. Liang, F.P. Sun, C.A. Rogers, Coupled electromechanical analysis of adaptive material systems–determination of the actuator power consumption and system energy transfer, J. Intell. Mater. Syst. Struct. 5 (1994) 12–20.
[24] G. Park, H. Sohn, C.R. Farrar, D.J. Inman, Overview of piezoelectric impedance-based health monitoring and path forward, Shock Vib. Dig. 35 (2003) 451–463.
[25] W.S. Na, J. Baek, A review of the piezoelectric electromechanical impedance based structural health monitoring technique for engineering structures, Sensors 18 (2018) 1307.
[26] R. Tawie, H.K. Lee, Piezoelectric-based non-destructive monitoring of hydration of reinforced concrete as an indicator of bond development at the steel-concrete interface, Cem. Concr. Res. 40 (2010) 1697–1703.
[27] V.G.M. Annamdas, Y. Yang, C.K. Soh, Impedance based concrete monitoring using embedded PZT sensors, Int. J. Civ. Struct. Eng. 1 (2010) 414–424.
[28] D. Xu, X. Cheng, S. Huang, M. Jiang, Identifying technology for structural damage based on the impedance analysis of piezoelectric sensor, Constr. Build. Mater. 24 (2010) 2522–2527.
[29] B.S. Divsholi, Y. Yang, Combined embedded and surface-bonded piezoelectric transducers for monitoring of concrete structures, NDT & E Int. 65 (2014) 28–34.
[30] V. Talakokula, S. Bhalla, R.J. Ball, C.R. Bowen, G.L. Pesce, R. Kurchania, B. Bhattacharjee, A. Gupta, K. Paine, Diagnosis of carbonation induced corrosion initiation and progression in reinforced concrete structures using piezo-impedance transducers, Sens. Actua. A 242 (2016) 79–91.
[31] B.K. Panker, A.R. Khedikar, Reinforcement corrosion assessment using PZT sensors via electro mechanical impedance technique, J. Emerging Technol. Innov. Res. 5 (2018) 149–152.
[32] W. Li, T. Liu, D. Zou, J. Wang, T.H. Yi, PZT based smart corrosion coupon using electromechanical impedance, Mech. Sys. Signal Proc. 129 (2019) 455–469.
[33] D. Xu, S. Banerjee, Y. Wang, S. Huang, X. Cheng, Temperature and loading effects of embedded smart piezoelectric sensor for health monitoring of concrete structures, Constr. Build. Mater. 76 (2015) 187–193.
[34] S.N. Khante, S.R. Gedam, PZT based smart aggregate for unified health monitoring of RC structures, Open J. Civil Eng. 6 (2016) 42–49.
[35] D. Ai, H. Zhu, H. Luo, Sensitivity of embedded active PZT sensor for concrete structural impact damage detection, Constr. Build. Mater. 111 (2016) 348–357.
[36] A. Dixit, S. Bhalla, Prognosis of fatigue and impact induced damage in concrete using embedded piezo-transducers, Sens. Actua. A 274 (2018) 116–131.
[37] A. Narayanan, A. Kocherla, V.L. Kolluru, K.V.L. Subramania, Understanding the coupled electromechanical response of a PZT patch attached to concrete: Influence of substrate size, Measurement 124 (2018) 505–514.
[38] J. Zhang, C. Zhang, J. Jiao, J. Jiang, A PZT-Based Electromechanical Impedance Method for Monitoring the Soil Freeze-Thaw Process, Sensors 19 (2019) 1107.
[39] L. Qin, Z.J. Li, Monitoring of cement hydration using embedded piezoelectric transducers, Smart Mater. Struct. 17 (2009) 055005.
[40] S. Liu, J. Zhu, S. Seraj, R. Cano, M. Juenger, Monitoring setting and hardening of mortar and concrete using ultrasonic shear waves, Constr. Build. Mater. 72 (2014) 248–255.
[41] G. Trtnik, M. Gams, Ultrasonic assessment of initial compressive strength gain of cement based materials, Cem. Concr. Res. 67 (2015) 148–155.
[42] Y.Y. Lim, K.Z. Kwong, W.Y.H. Liew, C.K. Soh, Non-destructive concrete strength evaluation using smart piezoelectric transducer—a comparative study, Smart Mater. Struct. 25 (2016) 085021.
[43] Y.Y. Lima, S.T. Smith, C.K. Soh, Wave Propagation based monitoring of concrete curing using piezoelectric materials: review and path forward, NDT & E Int. 99 (2018) 50–63.
[44] S.W. Shin, A.R. Qureshi, J.Y. Lee, C.B. Yun, Piezoelectric sensor based nondestructive active monitoring of strength gain in concrete, Smart Mater. Struct. 17 (2008) 055002.
[45] S.W. Shin, T.K. Oh, Application of electro-mechanical impedance sensing technique for online monitoring of strength development in concrete using smart PZT patches, Constr. Build. Mater. 23 (2009) 1185–1188.
[46] D. Wang, H. Zhu, Monitoring of the strength gain of concrete using embedded PZT impedance transducer, Constr. Build. Mater. 25 (2011) 3703–3708.
[47] T.J. Saravanan, K. Balamonica, C.B. Priya, N. Gopalakrishnan, S.G.N. Murthy, Piezoelectric EMI-based monitoring of early strength gain in concrete and damage detection in structural components, J. Infrastruct. Syst. 23 (2017) 04017029.
[48] A. Kocherla, A. Narayanan, K.V.L. Subramaniam, Monitoring progressive changes in cementitious materials using embedded piezo-sensors, Proc. SPIE 10170 (2017) 101702I.
[49] X. Lu, Y.Y. Lim, C.K. Soh, A Novel electromechanical impedance-based model for strength development monitoring of cementitious materials, Struct. Health Monit. 17 (2018) 902–918.
[50] E. Ghafri, Y. Yuan, C. Wu, T. Nantung, N. Lu, Evaluation the compressive strength of the cement paste blended with supplementary cementitious materials using a piezoelectric-based sensor, Constr. Build. Mater. 171 (2018) 504–510.
[51] Y.F. Su, G. Han, A. Amran, T. Nantung, N. Lu, Instantaneous monitoring the early age properties of cementitious materials using PZT-based electromechanical impedance (EMI) technique, Constr. Build. Mater. 225 (2019) 340–347.
[52] Z.J. Li, D. Zhang, K.R. Wu, Cement-based 0–3 Piezoelectric composites, J. Am. Ceram. Soc. 85 (2002) 305–313.
[53] B. Dong, Z.J. Li, Cement-based piezoelectric ceramic smart composites, Compos. Sci. Technol. 65 (2005) 1363–1371.
[54] D. Xu, X. Cheng, S. Huang, M. Jiang, Electromechanical properties of 2–2 cement based piezoelectric composite, Curr. Appl. Phys. 9 (2009) 816–819.
[55] D. Xu, S. Huang, X. Cheng, Electromechanical impedance spectra investigation of impedance-based PZT and cement/polymer based piezoelectric composite sensors, Constr. Build. Mater. 65 (2014) 543–550.
[56] J. Zhang, Y. Lu, Z. Lu, C. Liu, G. Sun, Z. Li, A new smart traffic monitoring method using embedded cement-based piezoelectric sensors, Smart Mater. Struct. 24 (2015) 025023.
[57] X. Cheng, S. Huang, J. Chang, R. Xu, F. Liu, L. Lu, Piezoelectric and dielectric properties of piezoelectric ceramic–sulphoaluminate cement composites, J. Euro. Ceram. Soc. 25 (2005) 3223–3228.
[58] S. Huang, J. Chang, L. Lu, F. Liu, Z. Ye, X. Cheng, Preparation and polarization of 0–3 cement based piezoelectric composites, Mater. Res. Bull. 41 (2006) 291–297.
[59] A. Chaipanich, N. Jaitanong, T. Tunkasiri, Fabrication and properties of PZT–ordinary portland cement composites, Mater. Lett. 61 (2007) 5206–5208.
[60] H. Gong, Y. Zhang, J. Quan, S. Che, Preparation and properties of cement based piezoelectric composites modified by CNTs, Curr. Appl. Phys. 11 (2011) 653–656.
[61] F. Wang, H. Wang, Y. Song, H. Sun, High piezoelectricity 0–3 cement-based piezoelectric composites, Mater. Lett. 76 (2012) 208–210.
[62] H.H. Pan, D.H. Lin, R.H. Yang, High Piezoelectric and dielectric properties of 0–3 PZT/cement composites by temperature treatment, Cem. Conc. Compos. 72 (2016) 1–8.
[63] H.H. Pan, R.H. Yang, Y.C. Cheng, High piezoelectric properties of cement piezoelectric composites containing kaolin, Proc. SPIE 9437 (2015) 94370R.
[64] H.H. Pan, C.K. Wang, Y.C. Cheng, Curing time and heating conditions for piezoelectric properties of cement-based composites containing PZT, Constr. Build. Mater. 129 (2016) 140–147.
[65] H.H. Pan, C.K. Wang, M. Tia, Y.M. Su, Influence of water-to-cement ratio on piezoelectric properties of cement-based composites containing PZT particles, Constr. Build. Mater. 239 (2020) 117858.
[66] B. Dong, F. Xing, Z.J. Li, Electrical response of cement-based piezoelectric ceramic composites under mechanical loadings, Smart Mater. Res. 2011 (2011) 236719.

[67] F.Z. Wang, H. Wang, H.J. Sun, S.G. Hu, Research on a 0–3 cement-based piezoelectric sensor with excellent mechanical–electrical response and good durability, Smart Mater. Struct. 23 (2014) 045032.
[68] L. Qin, Y. Lu, Z. Li, Embedded Cement-Based Piezoelectric Sensors for Acoustic Emission Detection in Concrete, J. Mater. Civ. Eng. 22 (2010) 1323–1327.
[69] Y. Lu, Z. Li, Frequency characteristic analysis on acoustic emission of mortar using cement-based piezoelectric sensors, Smart Struct. Sys. 8 (2011) 321–341.
[70] Y. Lu, J. Zhang, Z. Li, B. Dong, Corrosion monitoring of reinforced concrete beam using embedded cement-based piezoelectric sensor, Mag. Conc. Res. 65 (2013) 1265–1276.
[71] H. Zhou, Y. Liu, Y. Lu, P. Dong, B. Guo, W. Ding, F. Xing, T. Liu, B. Dong, In-situ crack propagation monitoring in mortar embedded with cement-based piezoelectric ceramic sensors, Constr. Build. Mater. 126 (2016) 361–368.
[72] H.H. Pan, Y.D. Wong, Y.M. Su, Piezoelectric cement sensor and impedance analysis for concrete health monitoring, Proc. SPIE 10971 (2019) 109710Y.
[73] A. Chaipanich, R. Rianyoi, R. Potong, N. Jaitanong, Aging of 0–3 piezoelectric PZT ceramic-Portland cement composites, Ceram. Int. 40 (2014) 13579–13584.
[74] H.H. Pan, C.K. Chiang, Effect of aged binder on piezoelectric properties of cement-based piezoelectric composites, Acta Mech. 225 (2014) 1287–1299.
[75] S. Bhalla, C. Soh, Structural Health Monitoring by Piezo-Impedance Transducers, J. Aero. Eng. 17 (2004) 154–165.
[76] A. Narayanan, A. Kocherla, K.V.L. Subramaniam, Embedded PZT sensor for monitoring mechanical impedance of hydrating cementitious materials, J. Nondestruct. Eval. 36 (2017) 64.
[77] X. Lu, Y.Y. Lim, I. Izadgoshasb, C.K. Soh, Strength development monitoring and dynamic modulus assessment of cementitious materials using EMI-Miniature Prism based technique, Struct. Health Monitoring May (2019) 20.